Mon. Not. R. Astron. Soc. **322**, 343–355 (2001)

Dynamical evolution of the Prometheus–Pandora system

F. Poulet[1,2★†] and B. Sicardy[1]

[1]*DESPA, Observatoire de Paris, 5 Place Jules Janssen, 92195 Meudon, France*
[2]*NASA Ames Research Center, MS 245-3 Moffett Field, 94035 CA, USA*

Accepted 2000 October 2. Received 2000 August 31; in original form 1999 December

ABSTRACT

The system of Saturn's inner satellites is saturated with many resonances. Its structure should be strongly affected by tidal forces driving the satellites through several orbit–orbit resonances. The evolution of these satellites is investigated using analytic and numerical methods. We show that the pair of satellites Prometheus and Pandora has a particularly short lifetime ($<$20 Myr) if the orbits of the satellites converge without capture into a resonance. The capture of Pandora into a resonance with Prometheus increases the lifetime of the couple by a few tens of Myr. However, resonances of the system are not well separated, and capture results in a chaotic motion. Secondary resonances also disrupt the resonant configurations. In all cases, the converging orbits of these two satellites result in a close encounter. The implications for the origin of Saturn's rings are discussed.

Key words: celestial mechanics – planets and satellites: individual: Saturn.

1 INTRODUCTION

The orbital evolution of planetary satellites is governed primarily by tidal interactions between the satellites and the central planet, and by their mutual gravitational interactions. The dynamics is relatively well known for the systems of Uranus (Dermott, Malhotra & Murray 1988; Tittemore & Wisdom 1988; Tittemore & Wisdom 1989; Duncan & Lissauer 1997) and of Neptune (Banfield & Murray 1992). For the system of Saturn, an additional effect, stemming from the resonant interactions between the satellites and the main rings, raises numerous problems concerning the evolution of the small inner satellites. This paper addresses the question of the tidal evolution and mutual interactions between the small inner satellites of Saturn.

These satellites, with radii of only 15 to 89 km are smaller than Mimas (radius $\sim$200 km), and are difficult to observe from the Earth because they orbit close to Saturn's bright rings, at distances ranging from 2.2 to 2.5 Saturn radii. Discovered with ground-based telescopes during the 1966 and 1980 Saturn ring plane crossings and by the *Voyager* 1 and 2 spacecraft, these small satellites include Pan, orbiting within the Encke gap, Atlas, just outside the outer edge of the A ring, the two F ring shepherds (Prometheus and Pandora) and the two co-orbital satellites (Janus and Epimetheus). Prometheus, Pandora, Janus, Epimetheus and Mimas are responsible for numerous resonant spiral waves observed in the main rings, which in turn result in a significant transfer of angular momentum from the rings to the satellites (Goldreich & Tremaine 1982). As external satellites extract angular momentum, their orbits expand. Calculations based on the formula for the linear satellite torque predict remarkably short time-scales ($\leq 100 \times 10^8$ yr) for the orbital evolution of the satellites (Lissauer, Peale & Cuzzi 1984; Lissauer, Goldreich & Tremaine 1985).

The latest crossings of the Earth and Sun through Saturn's ring plane in 1995–96 have provided the best opportunity to observe Saturn's small inner satellites from Earth until the year 2004 when the Cassini orbiter will start its exploration of the saturnian system. The combined analysis of Voyager observations in 1980–81 and those of the *Hubble Space Telescope* (*HST*) in 1995–96, together with several ground-based telescopes (Nicholson et al. 1996), showed a surprising Prometheus' lag of about 19° with respect to its expected position. Subsequent *HST* observations made in 1996, 1997 and 1998 showed that this lag is increasing by approximately 0.6 deg yr^{-1} (French et al. 1998). French et al. (1999) discovered that Pandora's mean motion was $\sim$4 deg yr^{-1} less than expected, corresponding to an increase in the semimajor axis of 1.8 km. These lags, larger than the predicted lags from the back-reaction from the ring tidal torques, complicate the time-scale problem for the F ring satellites. However, previous and current investigations (Murray & Giuliatti Winter 1996; Dones et al. 1999; Showalter, Dones & Lissauer 1999) indicate that these lags could be due to short-term interactions with the F ring for Prometheus and with Mimas for Pandora. As the goal of our research is to understand the long-term dynamics (several tens of Myr), we study the orbits of the small satellites affected only by the long-term effects due to the tidal torques, and to their mutual interactions.

Two mechanisms have been considered to reduce the outward evolution of satellites. Since angular momentum may be transferred outward in resonant interactions between satellites, the small inner satellites could be locked in orbital resonances

★ Now at NASA Ames.
† E-mail: poulet@cosmic.arc.nasa.gov

with Saturn's outer moons. However, Prometheus and the co-orbital satellites are not near any low-order resonance with an outer moon at the present time. Only the outward motion of Pandora could be reduced, because it is extremely close to a 3:2 commensurability with Mimas (Borderies, Goldreich & Tremaine 1984). The effect of this commensurability was recently discovered. *HST* observations between 1996 and 2000 reveal that a periodic signature in Pandora's mean longitude with an amplitude of about 0.8 deg and a period of 580 d is superimposed on the slow drift (French et al. 1999). While this drift, like that of Prometheus, is unexplained, the oscillatory component matches both in amplitude and phase the expected perturbation due to the nearby 3:2 corotation resonance with Mimas (Dones et al. 1999). However, as discussed later, this effect should be only transient and not affect the long-term dynamics which is studied in this paper. A second mechanism which could reduce the orbital expansion is that the angular momentum transfer might be overestimated, but this has not been proved yet.

Another possibility for increasing the lifetime of this ring–satellite system is presented in this paper. It involves the resonant configurations encountered by the inner satellites with time. It is generally accepted that numerous resonances between large satellites have been established because of the tidal effect due to the planet, which causes the orbits of the satellites to expand with rates proper to each satellite (Goldreich 1965). When two satellites orbitally evolve through an isolated mean motion resonance, the outcome depends upon whether their orbits are converging or diverging. If the orbits of two bodies are diverging as they evolve, both resonant and tidal effects are additive and resonance trapping does not occur. For converging orbits, a resonant configuration can be maintained. We will see that this phenomenon is particularly rapid for the pair Pandora–Prometheus. Under the effect of a large orbital expansion, Prometheus can overtake Pandora in less than 20 Myr. However, we will also see that the presence of numerous mutual resonances can yield a capture into resonance, which would increase significantly their lifetime.

In this work, we consider the density wave torques on Saturn's inner satellites. We use both analytic techniques and numerical integrations to characterize probable evolution routes of this multiple ring–satellite system. The combination of these complementary approaches is very helpful, because the theoretical analysis provides a classification of the general outcomes of idealized cases (single-resonance theory), while the numerical method reveal the complexities of the full dynamics. In Section 2 the changes in the satellite orbital radii are considered, and it is shown that Prometheus and Pandora have very unusual dynamical behaviours. The analytic and numerical approaches used to study the dynamics of Prometheus and Pandora are described in Sections 3, 4 and 5, and then compared in Section 6. Finally, the lifetime of the system is discussed (Section 7), and the consequences of this evolution on the formation of Saturn's rings are investigated (Section 8).

2 PROMETHEUS AND PANDORA: AN UNUSUAL PAIR OF SATELLITES

The attraction of the tidal bulge raised on a planet by a satellite outside the synchronous orbit results in a gain of angular momentum by the satellite. This causes the orbit of the satellite to expand. The rate of change of the semimajor axis a of a satellite (mass m, orbital velocity Ω) with time is then

$$\left(\frac{\dot{a}}{a}\right)_{\rm t} = 3\left(\frac{G}{M_{\rm P}}\right)^{1/2} k_{2\rm P}\frac{R_{\rm P}^5}{Q_{\rm P}}\frac{m}{a^{13/2}}, \quad (1)$$

where $M_{\rm P}$, $R_{\rm P}$, $Q_{\rm P}$ and $k_{2\rm P}$ are the mass, the radius, the dissipation factor and the Love number of the planet (Burns 1977). The last parameter can be related to the dynamical oblateness J_2 through $k_{2\rm P} = 4\pi G\rho_{\rm P} J_2 \Omega_{\rm P}^{-2}$, where $\rho_{\rm P}$ and $\Omega_{\rm P}$ are the mass density and the spin rate of the planet. The orbital history of the satellites remains generally uncertain because of the lack of knowledge of the dissipation factor $Q_{\rm P}$ and the mass of the satellites.

For the system of Saturn, the evolution of the small moons near the rings is unique, because the waves resonantly driven in the rings transfer angular momentum to the moons. Under the conditions $\frac{a-r}{a} \ll 1$ and $\frac{(a-r)^2}{a^2} \ll \frac{\Delta r}{a} \ll \frac{a-r}{a}$, the rate of change of the semimajor axis a of a satellite due to the exchange of angular momentum with a part of ring (mean radius r, width Δr, surface density σ) is given by (Goldreich & Tremaine 1982)

$$\left(\frac{\dot{a}}{a}\right)_{\rm t} \approx 0.8\,\frac{2\pi r\Delta r\sigma m}{M_{\rm P}^2}\left(\frac{a}{a-r}\right)^4 \Omega. \quad (2)$$

Note that the variation in the eccentricity e of a satellite from these tidal effects is quite negligible during the time-scales considered here (less than 100 Myr).

Most of the resonances between the inner satellites and the rings are located in the A ring. The density waves give an estimation of the ring surface mass density of about $\sigma = 40\,{\rm g\,cm^{-3}}$ (Rosen et al. 1991). The values of the parameters of Saturn and of its inner satellites are listed in Tables 1 and 2. Note that we use the orbital elements as derived from the 1980/81 Voyager observations and not the most recent results of French et al. (1998, 1999). A comparison of expansion rates given by equations (1) and (2) shows that the effect of the A ring is considerably larger than the tidal effect due to the planet for all the satellites inside the orbit of Mimas (for instance, it is ~1000 times larger for Prometheus).

If the orbital expansion is playing a significant role, then equation (2) gives an upper limit for the age of the satellites. Prometheus (Pandora) should have been at the outer edge of the rings within the past 10 Myr (70 Myr) for a density of $\rho = 1.2\,{\rm g\,cm^{-3}}$. In

Table 1. Physical parameters of Saturn.

$GM_{\rm P}$† (km^3 s^{-2})	3.7931272×10^7
$R_{\rm P}$† (km)	60330
J_2†	16298×10^{-6}
$k_{2\rm P}$‡	0.3
$Q_{\rm P}$‡	$>1.6 \times 10^4$

† Campbell & Anderson (1989)
‡ Dermott et al. (1988)

Table 2. Physical parameters of small inner satellites.

Satellite	a (km)	m (g)	Ω (rad s^{-1})
Mimas†	185480	4.548×10^{22}	0.772×10^{-4}
Janus‡	151503	1.980×10^{21}	1.046×10^{-4}
Pandora§	141712	$*4.358 \times 10^{20}$	1.157×10^{-4}
Prometheus§	139377	$*6.542 \times 10^{20}$	1.186×10^{-4}

† Cuzzi et al. (1984)
‡ Nicholson et al. (1992)
§ Synnott et al. (1983)
*assuming a density of $1.2\,{\rm g\,cm^{-3}}$

addition, since the expansion rate is proportional to m and to $a^{5/2}/(a-r)^4$, the orbit of the inner and most massive satellite Prometheus will expand more rapidly than that of Pandora, so that their orbits are expected to converge with time in the absence of interactions with other satellites.

At present, these predicted rapid time-scales for orbital evolution due to resonant torques are purely theoretical, and they have not yet been confirmed by observations. However, the density waves have been observed at places predicted by the theory, and the torques are only a direct consequence of these gravitational interactions.

If the ring–satellite interactions seem to be a physical reality, there remains some uncertainty with the quantitative derivation of torques, and so, with the orbital expansion rate. First, the imprecise knowledge of satellite masses makes it difficult to determine the exact values of the torques. However, the fact that Prometheus is more massive than Pandora is likely to be robust due to the difference in size. This, combined with the fact that Prometheus is closer of the rings, ensures the orbital converging. As suggested in the introduction, the standard torque could be less efficient than estimated by the linear theory either because of the formation of gaps at resonant locations (Goldreich & Tremaine 1982) or because of non-linear effects (Brophy et al. 1992). However, no gap was detected, while the second suggestion remains unproven.

Note finally that we do not consider the effect of the F ring located between Prometheus and Pandora on the evolution of these small satellites. If the F ring is massive, an exchange of angular momentum with the satellites is possible. In addition, Murray & Giuliatti Winter (1996) have suggested that there could have some collisions between Prometheus and the F ring leading to the lag (Nicholson et al. 1996). So the F ring might have a large influence on the orbital evolution of this satellite. However, this is located in a very chaotic zone, which causes the particles to have short lifetimes of a few tens of thousand years (Poulet & Jancart 2000). This result confirms the works of Cuzzi & Burns (1988), Scargle et al. (1993) and Poulet et al. (2000), which show from different arguments the transitory character of the F ring with a lifetime of a few tens of thousand years at most. In addition, the dependence of the orbital evolution on satellite mass suggests that if the innermost body is the most massive, it will likely overtake and sweep up all exterior material.

In summary, the influence of the F ring on the shepherd satellites, and more particularly on Prometheus, seems actually non-negligible only in the short term. As suggested in the introduction, the study of the long-term evolution of these satellites can then be done without taking into account the interactions with the F ring.

The two satellites could be locked in orbital resonances with Saturn's other moons. In order to identify possible resonance crossings, Fig. 1 shows a model of the tidal evolution of the inner Saturnian satellites. We have plotted only first-order resonances, because these are the strongest ones. Because we are interested in explaining the evolution of Prometheus and Pandora, we have indicated only those involving these satellites. The evolution of Epimetheus was also ignored, since it shares Janus' orbit. The passages through resonances and the possible captures are discussed in Sections 4 and 6. However, it appears that the Prometheus/Pandora pair has an unusual evolution because their orbits converge rapidly, and also because they have encountered and will encounter numerous commensurabilities. On the other hand, we will see that the probability of capture of one of shepherd satellites in a first-order resonance associated with Janus or Mimas is only a few per cent. This probability, combined with the low number of resonances crossed (Fig. 1), implies that a capture by Janus or Mimas remains unlikely, and the effects of other inner

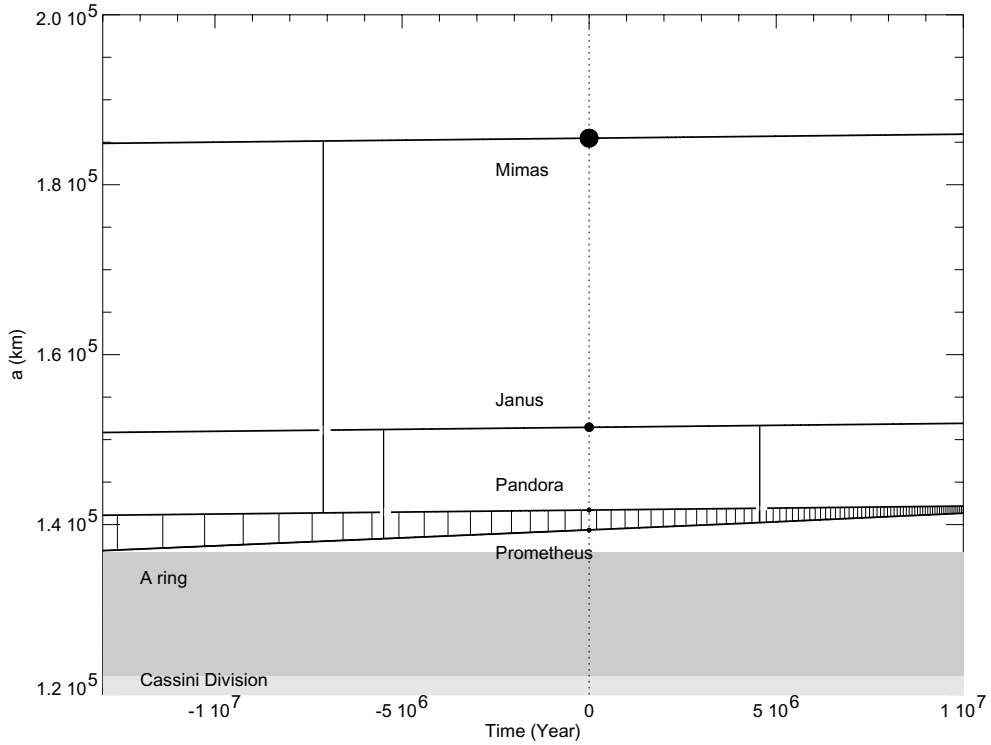

Figure 1. Variation of orbital radii with time due to tidal dissipation and ring torque. The first-order resonances that Prometheus and Pandora could encounter are marked with vertical lines. The origin of time corresponds to our epoch.

satellites on the pair are also unimportant. This explains why we restrict our study to the stability of the system Prometheus and Pandora, ignoring the interactions with the other satellites.

3 VARIATIONS OF ORBITAL ELEMENTS

To calculate the changes in the orbital elements, two approaches have been investigated: (1) an analytic method; (2) a numerical integration of orbits. The analytic approach uses the Lagrange's equations, which give the variations of the orbital elements of a satellite in the planar case:

$$\dot{a} = \frac{2}{na}\frac{\partial R}{\partial \lambda} + \dot{a}_t \tag{3}$$

$$\dot{n} = -\frac{3}{a^2}\frac{\partial R}{\partial \lambda} + \dot{n}_t \tag{4}$$

$$\dot{e} = -\frac{\sqrt{1-e^2}}{na^2e}(1-\sqrt{1-e^2})\frac{\partial R}{\partial \lambda} - \frac{\sqrt{1-e^2}}{na^2e}\frac{\partial R}{\partial \varpi} \tag{5}$$

$$\dot{\varpi} = \frac{\sqrt{1-e^2}}{na^2e}\frac{\partial R}{\partial e} \tag{6}$$

$$\dot{\epsilon} = -\frac{2}{na}\frac{\partial R}{\partial a} + \frac{\sqrt{1-e^2}}{na^2e}(1-\sqrt{1-e^2})\frac{\partial R}{\partial e}, \tag{7}$$

where the mean longitude λ is a function of the mean longitude at epoch ϵ: $\lambda = \int n\,dt + \epsilon$. The angle ϖ is the longitude of pericentre. The quantities $\dot{a}_t$ and $\dot{n}_t$ are the rates of change of the semimajor axis and of the mean motion due to tides. Note that we neglect the very small change in e due to the torques. Tidal dissipation in the satellites results in a change in the eccentricity, but for small bodies with radii $\leq$100 km that have the least complex thermal histories, no significant thermal activity occurs (Schubert, Spohn & Reynolds 1986). Thus we did not take into account this damping of eccentricity. R is the perturbing function (negative of the perturbing potential), composed of the functions $R_{\rm pert}$ due to the other satellite and R_{J_2} due to the planet's oblateness. The expression of $R_{\rm pert}$ can be Fourier-expanded in series containing resonant terms.[1] Below, we consider only the perturbations of Prometheus on Pandora, whose mass is neglected. If the subscripts $_{\rm pro}$ and $_{\rm pd}$ refer to Prometheus and Pandora, the expression for the perturbing function $R_{\rm pd}$ is then, to first-order in eccentricity,

$$R_{\rm pd} = -\frac{Gm_{\rm pro}}{2a_{\rm pd}}(A_1 e_{\rm pd}\cos\phi_1 + A_2 e_{\rm pro}\cos\phi_2) \tag{8}$$

with

$$\phi_1 = (p+1)\lambda_{\rm pro} - p\lambda_{\rm pd} - \varpi_{\rm pd}$$

$$\phi_2 = (p+1)\lambda_{\rm pro} - p\lambda_{\rm pd} - \varpi_{\rm pro}$$

$$A_1 = -(2p+1)b_{1/2}^{(p+1)} + \alpha\frac{{\rm d}b_{1/2}^{(p+1)}}{{\rm d}\alpha}$$

$$A_2 = 2pb_{1/2}^{(p)} - \alpha\frac{{\rm d}b_{1/2}^{(p)}}{{\rm d}\alpha}.$$

The resonant eccentric angles ϕ_1 and ϕ_2 are respectively called the Lindblad angle and the corotation angle, $b_\gamma^{(m)}$ define the Laplace coefficients, and $\alpha = a_{\rm pro}/a_{\rm pd}$. The integer p is negative here, because we are interested in the resonance exterior to the perturbing body. Note also that $\frac{A_1}{|p|} \sim \frac{8}{5}$ for large values of $|p|$.

The perturbing function due to Saturn's oblateness is (Foryta & Sicardy 1996, hereafter FS96)

$$R_{J_2} = \frac{1}{2}a_{\rm pd}^2 n_{\rm pd}^2 J_2\left(\frac{R_{\rm P}}{a_{\rm pd}}\right)^2\left(1+\frac{3}{2}e_{\rm pd}^2\right). \tag{9}$$

4 DYNAMICS OF ECCENTRIC RESONANCE

An elegant description of the capture process under the effect of a slow variation of the system energy, and applicable to the most common orbital resonances, is found in Henrard & Lemaître (1983). This analysis relies on the perturbing Hamiltonian, truncated to a single term containing the resonant term. The tidal dissipation causes a slow variation of one of the parameters in the Hamiltonian, which leads to a slow deformation of the phase-space (Peale 1986). When the satellite encounters a resonance, two outcomes are possible: capture into the resonance, or a mere crossing through the resonance. The probability of capture is examined in Section 4.4. If there is a capture, the slow deformation of the area within the trajectory corresponds to an increase of the eccentricity (Section 4.5). However, the physics of the capture is well described if two assumptions are verified.

(1) The motion is adiabatic, i.e., the area within the trajectory in the phase-space has to be an invariant of the motion. This condition is studied in Section 4.3.

(2) The resonances are well separated. This condition can be roughly quantified in terms of the libration widths (Section 4.2).

The evolution of each resonant argument is approximated by the perturbed pendulum equation. This will allow us to specify the two previous conditions and to predict the orbital evolution during a capture into resonance. The analytic results will be then compared with the orbital evolutions derived from numerical integrations (Section 6).

We will see that the condition of the 'well-separated' resonances will not always be satisfied. In this case, the single-resonance theory becomes inadequate to describe the passage through or capture into a resonance. In particular, we expect to identify significant chaotic zones surrounding low-order resonances, and to find that escape from a resonance could occur even after long periods of stability. In fact, we will find that all the orbital evolutions of Prometheus and Pandora are unstable.

4.1 Model of pendulum

A resonance occurs when one of the resonant angles is stationary. We restricted our study to the Lindblad eccentric angle, because the observed captures into resonance (Section 6) mainly imply this angle. Thus the perturbing function is limited to ϕ_1. From equation (8), we obtain the second time derivative of ϕ_1: $\ddot{\phi}_1 = (p+1)\dot{n}_{\rm pro} - p\dot{n}_{\rm pd} + (p+1)\ddot{\epsilon}_{\rm pro} - p\ddot{\epsilon}_{\rm pd} - \ddot{\varpi}_{\rm pd}$. The perturbations of Pandora on Prometheus being low, and neglecting the second derivatives in the right-hand member, we find:

$$\ddot{\phi}_1 = (p+1)\dot{n}_{{\rm pro}_t} - p\dot{n}_{\rm pd}, \tag{10}$$

where $\dot{n}_{{\rm pro}_t}$ defines the variation of the mean motion due to the ring torques. Combining the expression of $\dot{n}_{\rm pd}$ (equation 4) with equation (10), it follows that

$$\ddot{\phi}_1 = -3p^2 C n_{\rm pd} e_{\rm pd}\sin\phi_1 + F \tag{11}$$

[1] In this work, we investigate the effects of mean motion eccentric resonances only, but note that the other classes of resonances (inclined for instance) may also be important.

with

$$C = \frac{Gm_{\rm pro}A_1}{2n_{\rm pd}a_{\rm pd}^3}$$

$$F = (p+1)\dot{n}_{\rm pro_t} - p\dot{n}_{\rm pd_t}.$$

Equation (11) is the perturbed pendulum equation. It defines the motion of the resonant angle for eccentricities larger than a critical value, derived in equation (13). The different motions of ϕ_1 can then be described in the phase-space $(\phi_1, \dot{\phi}_1)$. There is a libration of ϕ_1, which is separated from circulation by the separatrix that passes through the unstable equilibrium point. The variation of the energy of the system due to the tidal effects slowly modifies the phase-space, allowing transition from circulation to libration, i.e., capture.

Equation (11) was obtained by assuming that $\ddot{\epsilon}_{\rm pd}$ and $\ddot{\varpi}_{\rm pd}$ are negligible. Now, by combining equations (6), (7) and (8), we have, to lowest order in eccentricity,

$$\ddot{\varpi}_{\rm pd} = \frac{C^2}{2}\frac{1}{e_{\rm pd}^2}\sin 2\phi_1$$

$$\ddot{\epsilon}_{\rm pd} = -\frac{C^2}{4}\sin 2\phi_1.$$

Since $\ddot{\varpi}_{\rm pd} \approx \ddot{\epsilon}_{\rm pd}/e_{\rm pd}^2$, the term $\ddot{\varpi}_{\rm pd}$ will always dominate $\ddot{\epsilon}_{\rm pd}$, which can be ignored. Furthermore, for small eccentricity, we have

$$\ddot{\phi}_1 = -3p^2Cn_{\rm pd}e_{\rm pd}\sin\phi_1 - \frac{C^2}{2}\frac{1}{e_{\rm pd}^2}\sin 2\phi_1 + F. \qquad (12)$$

The variations of ϕ_1 will then be dominated by $\ddot{\varpi}_{\rm pd}$ only if the eccentricity is lower than

$$(e_{\rm pd})_{\rm crit} \sim \left(\frac{4}{15|p|}\frac{Gm_{\rm pro}}{n_{\rm pd}^2a_{\rm pd}^3}\right)^{1/3}, \qquad (13)$$

which implies $(e_{\rm pd})_{\rm crit} < 2\times10^{-4}$ for $|p| > 40$. This critical eccentricity, one order smaller than the actual value of eccentricities of Pandora, means that the contributions due to $\ddot{\varpi}_{\rm pd}$ and $\ddot{\epsilon}_{\rm pd}$ can actually be neglected, thus validating equation (11).

4.2 Width of a resonance

The maximum libration of ϕ_1 determined by the separatrix gives the boundaries of all values of a and e for which the trajectory is said to be in resonance. For a pendulum given by equation (11) without the tidal effect, the maximum deviation of mean motion from the exact commensurability of the mean motions is (Dermott & Murray 1983)

$$\Delta n_{\rm pd} = \pm\sqrt{12n_{\rm pd}|C|e_{\rm pd}}.$$

From Kepler's third law, the corresponding variation in semimajor axis is $\Delta a_{\rm pd} = -\frac{2}{3}\frac{a_{\rm pd}}{n_{\rm pd}}\Delta n_{\rm pd}$. Considering large values of $|p|$, which simplifies the expression of C, one gets

$$W_{\rm lib} \sim \frac{4}{3}\frac{a_{\rm pd}}{n_{\rm pd}}|\Delta n_{\rm pd}| \sim \frac{16}{\sqrt{15}}a_{\rm pd}\sqrt{|p|\frac{m_{\rm pro}}{M_{\rm P}}e_{\rm pd}}. \qquad (14)$$

The width of the resonance depends both on the mass ratio of the secondary to the primary and on the square root of the eccentricity. For any eccentricity lower than $(e_{\rm pd})_{\rm crit}$, $\ddot{\varpi}_{\rm pd}$ is no longer negligible. In this case, $W_{\rm lib}$ is obtained by considering the expression of the maximum variation of $\Delta n_{\rm pd}$ given by Winter & Murray (1997). We have computed the variations of libration widths for the system Prometheus–Pandora, and the results are shown in Fig. 2. The continuous lines show the parabolic shape resulting from including the effects due to small e. For very small eccentricities, the dotted lines indicate that the resonances overlap.

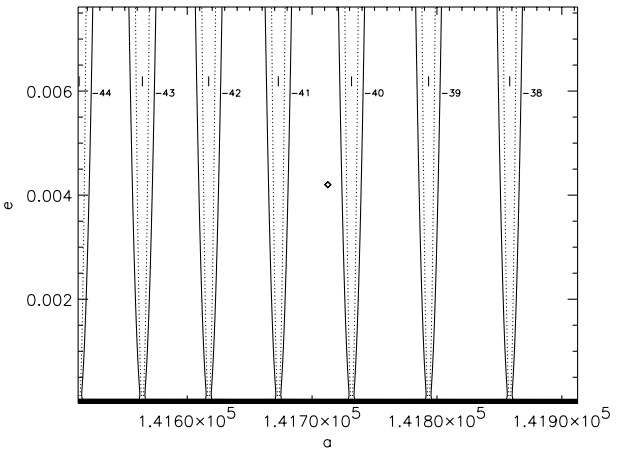

Figure 2. Libration regions in (a, e) space derived using the pendulum approach for different Lindblad resonances. The dashed line is the libration width derived by neglecting the pericentre contribution, and the solid line includes this contribution. The locations of the nominal semimajor axes are indicated at the top of the diagram. Pandora is located by the diamond. There is no overlap of the libration regions. The V-shapes move following the expansion rate of Prometheus, which is larger than that of Pandora. Therefore, Pandora will be overtaken by the Lindblad resonances.

The resonances are pushed outward according to the orbital expansion of Prometheus, which is larger than that of Pandora. The resonances will then overtake Pandora, so that this latter will encounter successively the resonances $p = -41, -42, \ldots$ in the future, with possible captures. The satellites will not remain in resonance if the disrupting effects of tidal forces are too strong. This phenomenon is quantified by evaluating the tidal effects on the evolution of the resonant angle. In a resonance, the angle ϕ_1 oscillates with amplitude less than 2π. For the resonance to be stable against the tidal effects, the sign of $\ddot{\phi}_1$ must change. Equation (11) then requires

$$F < 3p^2|C|n_{\rm pd}e_{\rm pd}.$$

Consequently, stability of a resonance against tidal dissipation is obtained for eccentricities larger than

$$(e_{\rm pd})_{\rm stab} = \frac{5}{12|p|^3}\frac{a_{\rm pd}^3}{Gm_{\rm pro}}F \approx 1\times10^{-7}, \qquad (15)$$

for $p = -40$. $(e_{\rm pd})_{\rm stab}$ is still lower for the other inner satellites. This raises the question: why is Pandora not in resonance with Prometheus or any other inner satellites? A possibility is that Pandora was captured, then ejected. However, its eccentricity is similar to those of other satellites, which probably means that it has never been captured into resonance. A clue will come from the estimation of the probability of capture, which is evaluated in Section 4.4.

4.3 Adiabatic criterion

The description of the resonant motion can be investigated if the

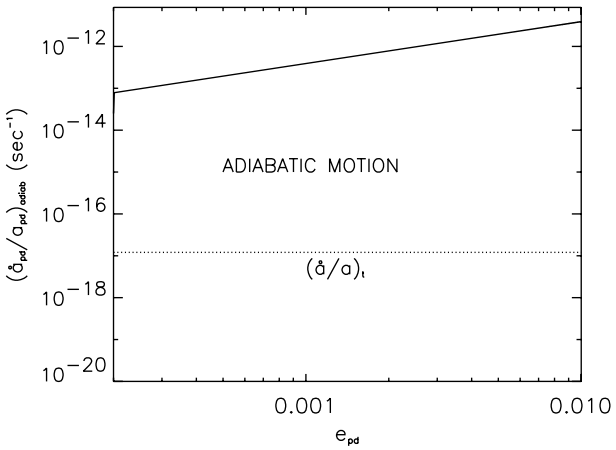

Figure 3. Criterion of the adiabatic motion. The rate of orbital expansion $(\dot{a}/a)_t$ (dotted line) is much lower than the critical value $(\dot{a}/a)_{adia}$ (continuous line) defined by the adiabatic criterion. Recall that this condition is valuable only for the eccentricities larger than $(e_{pd})_{crit}$ (equation 13).

tidal effects are not too important. More specifically, the rate $\left(\dot{a}_{pd}/a_{pd}\right)$ must satisfy an adiabatic criterion in the vicinity of the resonance. A minimal requirement is that the change in a produced by tides in one libration period T_{lib} is much smaller than the amplitude W_{lib} of the oscillations in a due to the first-order resonance:

$$(\dot{a}_{pd})_t \; T_{lib} \ll W_{lib}.$$

This condition defines a critical value of the rate of orbital expansion given by

$$\left(\frac{\dot{a}_{pd}}{a_{pd}}\right)_{adia} = \left(\frac{W_{lib}}{a_{pd} T_{lib}}\right). \tag{16}$$

Using the expression of T_{lib} given by Dermott et al. (1988), the adiabatic condition is shown in Fig. 3. The tidal rate (dotted line) is much smaller than the critical value (continuous line), so that the adiabatic condition is satisfied for the situation of interest. This allows use of the classical techniques of adiabatic invariant to derive the probability of capture into resonance.

4.4 Probability of capture

Passage through resonances has been much simplified by the work of Henrard & Lemaître (1983; See also Borderies & Goldreich 1984, Peale 1986 and Dermott et al. 1988). If the orbits of two bodies are diverging as they tidally evolve, both resonant and tidal effects are additive and resonance trapping does not occur. In this case, passage through the resonance results in a jump in eccentricity. For tidally converging orbits, a resonant configuration can be maintained under the following condition: the capture is certain if the resonance is encountered with an eccentricity lower than a critical value e_{capt}. For initial eccentricities higher than e_{capt}, capture into resonance is probabilistic. For example, Dermott et al. (1988) give the critical value of the eccentricity for which the capture is certain. In our case ($p \sim -40$), this gives

$$e_{capt} \sim \left\{ \frac{8\sqrt{6}\dfrac{m_{pro}}{M_P}}{5|p|\left[1 + \dfrac{m_{pd}}{m_{pro}}\left(\dfrac{a_{pro}}{a_{pd}}\right)^2\right]} \right\}^{1/3} \sim 5 \times 10^{-4}. \tag{17}$$

Pandora will encounter the resonance with a larger eccentricity. We have to introduce the probability of capture, whose expression is given below (Dermott et al. 1988):

$$P_c = 1 \;\text{ if }\; e_{pd} < e_{capt} \tag{18}$$

$$P_c \approx \frac{2}{3^{3/4}\pi}\left(\frac{e_{capt}}{e_{pd}}\right)^{3/2} \;\text{ if }\; e_{pd} > e_{capt}. \tag{19}$$

Considering the present eccentricity of Pandora, the probability of capture for Pandora is about 8×10^{-3}. So, this low probability allows us to understand better why Pandora is not in resonance with Prometheus in spite of the numerous resonances already encountered (Fig. 1).

The probability of capture in a first-order resonance associated with Janus or Mimas is a few per cent. So a capture by an inner satellite remains very unlikely in the future except for a capture by Prometheus.

4.5 Orbital evolution into resonance

The low probability derived previously does not exclude the possibility of a future capture, given the numerous resonances that Pandora will cross. Our numerical experiments will indeed show that it can occur (Section 6). The evolution of tidally evolving bodies once captured in resonance has been modelled by many past works (Peale 1986; Dermott et al. 1988). Here we just recall the expected evolutions of the semimajor axis and the eccentricity.

A capture into resonance means that the ratio of mean motions (here, n_{pd}/n_{pro}) remains constant in spite of continued expansion of the orbits from tidal interactions, i.e.,

$$\frac{1}{a_{pd}}\frac{da_{pd}}{dt} = \frac{1}{a_{pro}}\frac{da_{pro}}{dt}. \tag{20}$$

The eccentricity of a body is affected by its orbital energy and its angular momentum. From the Jacobi constant, the variation in eccentricity Δe is approximatively given by

$$e\Delta e \approx -\frac{\Delta E}{2E}.$$

Since E is negative, a gain of energy increases the eccentricity. A more rigorous approach can be done by using Lagrange's equations. In a resonance, the mean value of the second time derivative of the resonant argument is zero. From equation (11), we obtain $Ce_{pd}\langle \sin\phi_1 \rangle = F/3p^2 n_{pd}$, where $\langle\,\rangle$ denotes time average. To lowest order in the orbital elements, equation (5) becomes

$$\frac{\langle \dot{e}_{pd} \rangle}{e_{pd}} = \frac{F}{3p^2 n_{pd} e_{pd}^2}.$$

F being positive, the eccentricity increases, and the average evolution of e_{pd} in a resonance is

$$\langle e_{pd} \rangle = \sqrt{\frac{2}{3p^2}\frac{F}{n_{pd}}(t - t_0) + e_{0_{pd}}^2}, \tag{21}$$

where $e_{0_{pd}}$ is the initial eccentricity at time t_0 of the beginning of the capture.

5 NUMERICAL METHOD

The analytic model that describes the mutual perturbations between Prometheus and Pandora will be compared with numerical simulations. The classical numerical approach consists of integrating the equations of variation of the orbital elements given by equations (3)–(7). However, this method is numerically very slow. Moreover, the perturbation mainly occurs during a few revolutions around the conjunction. A possible approximation is to replace the effect of an encounter by an impulse. Such a method was used by FS96 in the study of the dynamics of Neptune's arcs. In this context, they developed a symplectic mapping, that provides the perturbations in the case of the restricted problem of three bodies. In this section we present the adaptation of the FS96 mapping for the system Pandora–Prometheus, which is a non-hierarchical system.

The general philosophy of the symplectic mapping is described in FS96. In the case of a satellite–particle system, the orbital elements of a particle are instantaneously changed at each conjunction with the satellite. FS96 give the expression of the transformation that provides the new orbital elements of the particle after an encounter as a function of the old ones. The mapping reproduces both the high-frequency terms arising from individual conjunctions, and the low-frequency terms associated with possible resonances. The variations of orbits are derived from Hill's equations. Their advantage is that they do not require any hypothesis about the mass ratios. Consequently, the processing of the relative motion remains valid for the non-hierarchical case. Below, we briefly present the implementation of the mapping which changes with respect to the mapping of FS96.

Let us define the usual complex eccentricities of the satellites, and of their centre of mass K:

$$\boldsymbol{p}_{\rm pro} \equiv e_{\rm pro} \exp(\mathrm{i}\varpi_{\rm pro})$$

$$\boldsymbol{p}_{\rm pd} \equiv e_{\rm pd} \exp(\mathrm{i}\varpi_{\rm pd})$$

$$\boldsymbol{p}_{\rm K} \equiv (1-\nu)\boldsymbol{p}_{\rm pro} + \nu \boldsymbol{p}_{\rm pd}.$$

Let us also define the average semimajor axis:

$$a_{\rm K} \equiv (1-\nu)a_{\rm pro} + \nu a_{\rm pd},$$

where $\nu = m_{\rm pd}/(m_{\rm pro} + m_{\rm pd})$. When $\nu \rightarrow 0$, we find the hierarchical case studied by FS96. The reduced complex eccentricity $\boldsymbol{p}_{\rm j}{}'$ of any satellite j is: $\boldsymbol{p}_{\rm j}{}' = (\boldsymbol{p}_{\rm j}/H)\exp(-\mathrm{i}\lambda_{\rm r})$, where $\lambda_{\rm r}$ is the common longitude of the two bodies at conjunction, and $H = \left(m_{\rm pro} + m_{\rm pd}/3M_{\rm P}\right)^{1/3}$ is the Hill coefficient. We finally deduce the parameters of the relative motion:

$$\boldsymbol{p}' = \frac{1}{H}(\boldsymbol{p}_{\rm pd} - \boldsymbol{p}_{\rm pro})\exp(-\mathrm{i}\lambda_{\rm r})$$

$$\delta = \frac{a_{\rm pd} - a_{\rm pro}}{R_{\rm H}}.$$

Here, $R_{\rm H} = Ha_K$ is the mutual Hill's radius of the interacting bodies. The FS96 mapping provides the variations of the impact parameter δ and the reduced complex eccentricity $\boldsymbol{p}'$. In particular, the value δ is taken so that the Jacobi constant is preserved. We then apply this mapping to get the new values. The new complex eccentricities and semimajor axis of the satellites are then:

$$\boldsymbol{p}_{\rm pro} \equiv \boldsymbol{p}_{\rm K} - \nu H \boldsymbol{p}' \exp(\mathrm{i}\lambda_{\rm r})$$

$$\boldsymbol{p}_{\rm pd} \equiv \boldsymbol{p}_{\rm K} + (1-\nu) H \boldsymbol{p}' \exp(\mathrm{i}\lambda_{\rm r})$$

$$a_{\rm pro} = a_{\rm K} - \nu R_{\rm H}\delta$$

$$a_{\rm pd} = a_{\rm K} + (1-\nu)R_{\rm H}\delta.$$

This gives the new orbital elements of the satellites.

The changes of the orbital elements given by this mapping must verify some conditions, which result from the development of Hill's equations. These conditions focus on the masses, the semimajor axes and the eccentricities of the satellites. Moreover, the treatment of an encounter under the impulse approximation implies that the orbital separation is larger than several Hill's radii. Knowing the physical elements of the satellites (Table 2), we verify that

(1) $\mu_{\rm pro}, \mu_{\rm pd} \ll 1$
(2) $a_{\rm pd} - a_{\rm pro} \ll a_{\rm pro}, a_{\rm pd}$
(3) $e_{\rm pro}a_{\rm pro}, e_{\rm pd}a_{\rm pd} < a_{\rm pd} - a_{\rm pro}$
(4) $a_{\rm pd} - a_{\rm pro} > 10R_{\rm H}$.

Because of these conditions, our simulations break down upon close approach between the shepherd satellites, and so our simulations are unable to track the evolution of the system until a physical collision occurs.

Far from a conjunction, the perturbations between satellites are negligible. However, between two conjunctions, the satellites undergo two types of perturbations which are due to the gravitational potential of the flattened planet and the tidal torques. The oblateness affects the precession of pericentre of each satellite as follows:

$$\dot{\varpi} = \left(\frac{GM_{\rm P}}{a^3}\right)^{1/2}\left[\frac{3}{2}\left(\frac{R_{\rm P}}{a}\right)^2 J_2 - \frac{15}{4}\left(\frac{R_{\rm P}}{a}\right)^4 J_4\right], \tag{22}$$

while the satellite mean motion is related to the mean geometric orbital radius through

$$n = \left(\frac{GM_{\rm P}}{a^3}\right)^{1/2}\left[1 + \frac{3}{4}\left(\frac{R_{\rm P}}{a}\right)^2 J_2\right] - \left(\frac{GM_{\rm P}}{a^3}\right)^{1/2}\left[\frac{9}{32}\left(\frac{R_{\rm P}}{a}\right)^4 J_2^2 + \frac{15}{16}\left(\frac{R_{\rm P}}{a}\right)^4 J_4\right]. \tag{23}$$

After each conjunction, and the application of the mapping, equations (22) and (23) provide the new values of orbital elements of each satellite.

For this work, the orbiting satellites are additionally accelerated by tidal torques at each time-step according to equations (1) and (2), even though the torque due to the planet tide is negligible. The torques also generate a decrease of the eccentricities, but this is much lower than the interactions induced by the gravitational perturbations between the satellites. Thus this effect is not included in our numerical simulations.

This mapping is used in the next section to integrate the motion of the Prometheus–Pandora pair in orbit around the flattened planet and undergoing the effects of tidal torques.

6 RESULTS: ORBITAL EXPANSION AND CAPTURE INTO RESONANCE

We classify our results in terms of evolutions without or with capture into resonance. All simulations presented here have been obtained for a satellite density of $1.2\,\mathrm{g\,cm^{-3}}$. The parameters used for these simulations are listed in Tables 1 and 2. As the densities are not well known, simulations have also been done with

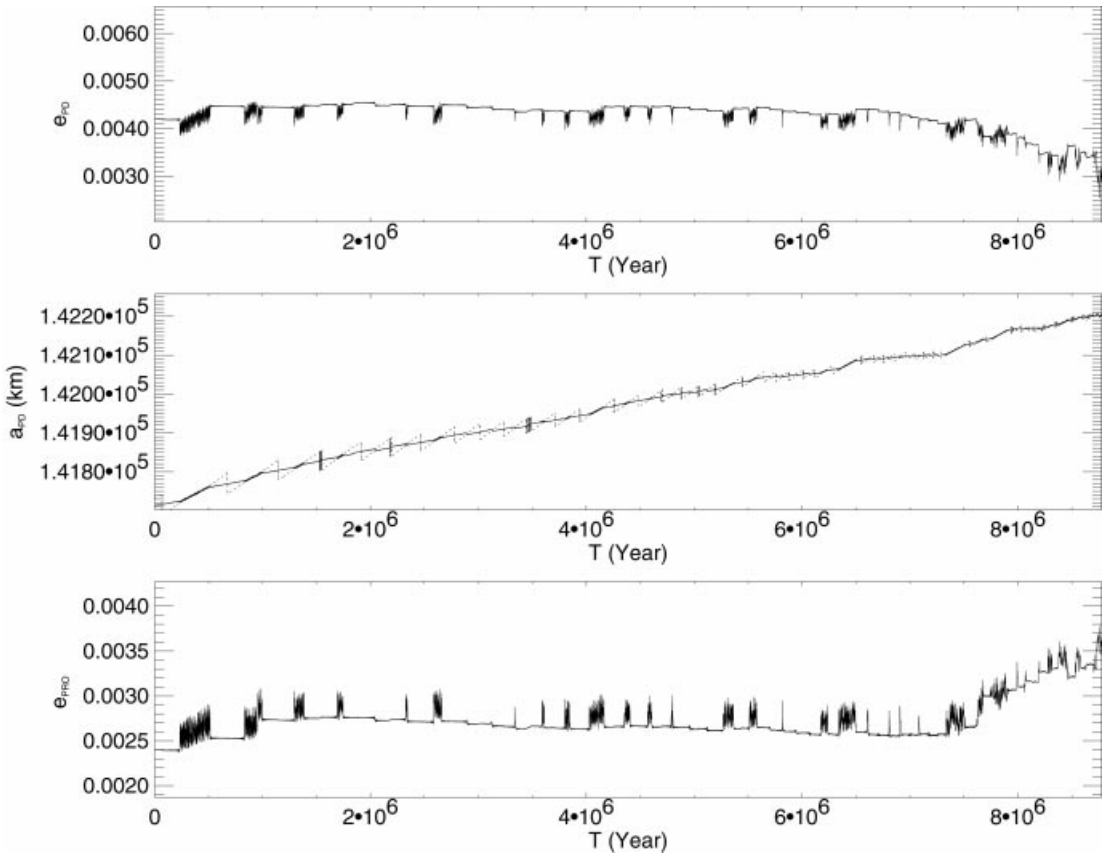

Figure 4. Variation of the eccentricities of Pandora $e_{\rm pd}$ (top panel) and Prometheus $e_{\rm pro}$ (bottom panel), and of the semimajor axis of Pandora $a_{\rm pd}$ (middle panel). This is a typical example of evolution without capture. In the middle panel, the drift $a_{\rm pd}$ (continuous line) is compared to the location of the closest Lindblad resonance to Pandora (dotted line). Pseudo-captures are detected when the dotted and continuous curves are superimposed. During such transient captures, one sees both the small excitation of the eccentricities and the increase of $a_{\rm pd}$ according the rate of Prometheus. They may be due to the proximity of the other resonances which creates a chaotic zone surrounding the separatrix. After about 9 Myr, there is a close encounter, and the numerical study is stopped because the mapping is no longer valid.

densities 50 per cent smaller. The results are qualitatively the same (Section 7). We launched a set of 40 runs with different values of the expansion tidal rate which verify the adiabatic criterion. The integrations were continued until Prometheus and Pandora experienced a very close encounter, at which point the mapping is no longer valid.

Evolution without capture: Fig. 4 shows the results of the numerical integration of the motions of Pandora and Prometheus. The orbital expansion of Prometheus is about 4 times larger than that of Pandora. Pandora encounters several resonances without being captured. Some transient captures occur, leading to a small excitation of the eccentricity. In fact, these excitations correspond to the passings through the chaotic zones surrounding the separatrix (J. M. Petit, personal communication). The drift of the semimajor axis of Pandora is compared with the drift of the closest Lindblad resonance to the satellite. The resonances, moving outward at the orbital rate of Prometheus, overtake Pandora. During transient captures, the orbital rates of Pandora and Prometheus are the same. Eventually, the orbits converge and the outcome of the evolution is a close encounter. This occurs in less than 10 Myr (or 20 Myr for a density of $0.6\,{\rm g\,cm^{-3}}$). The evolution without capture represents the majority of the evolutions (Section 7).

Evolution with capture: Fig. 5 shows the typical orbital evolutions during a capture of Pandora into a Lindblad resonance. The plotted parameters show features which are characteristic of first-order single-resonance capture (Section 4), namely: (1) an increase of the eccentricity of the captured satellite;[2] (2) the conservation of the semimajor axis ratio. However, the capture is not permanent. At time $T \approx 20 \times 10^6$ yr, Pandora escapes from the resonance. A second capture being very unlikely (Section 7), the evolution ends by a close encounter. In such an evolution, the time of the close encounter has been delayed by more than 10 Myr with respect to the evolution without capture.

Fig. 6 is the predicted evolution of $e_{\rm pd}$ (line) from the analytic formalism (equation 21) compared with the numerical results (points). We find that the increase is in good agreement with the analysis given above. Recall that the algebraic modelling is valid for well-separated resonances. The capture occurs for the $p = -59$ resonance that is indeed isolated from the neighbouring resonances for the given eccentricity of Pandora at time of capture, as shown in Fig. 7. This figure allows us to represent the set of resonances near Pandora as a function of time. When the radial separation of the two satellites diminishes, the resonances get closer together. The analytic modelling of the single resonance stays valid for $|p| < 65$. For larger values of $|p|$, we will see that the behaviour of Pandora is much more irregular.

[2] Note that the time-scale of the excitation of eccentricity is much shorter than that of the damping due to the tides.

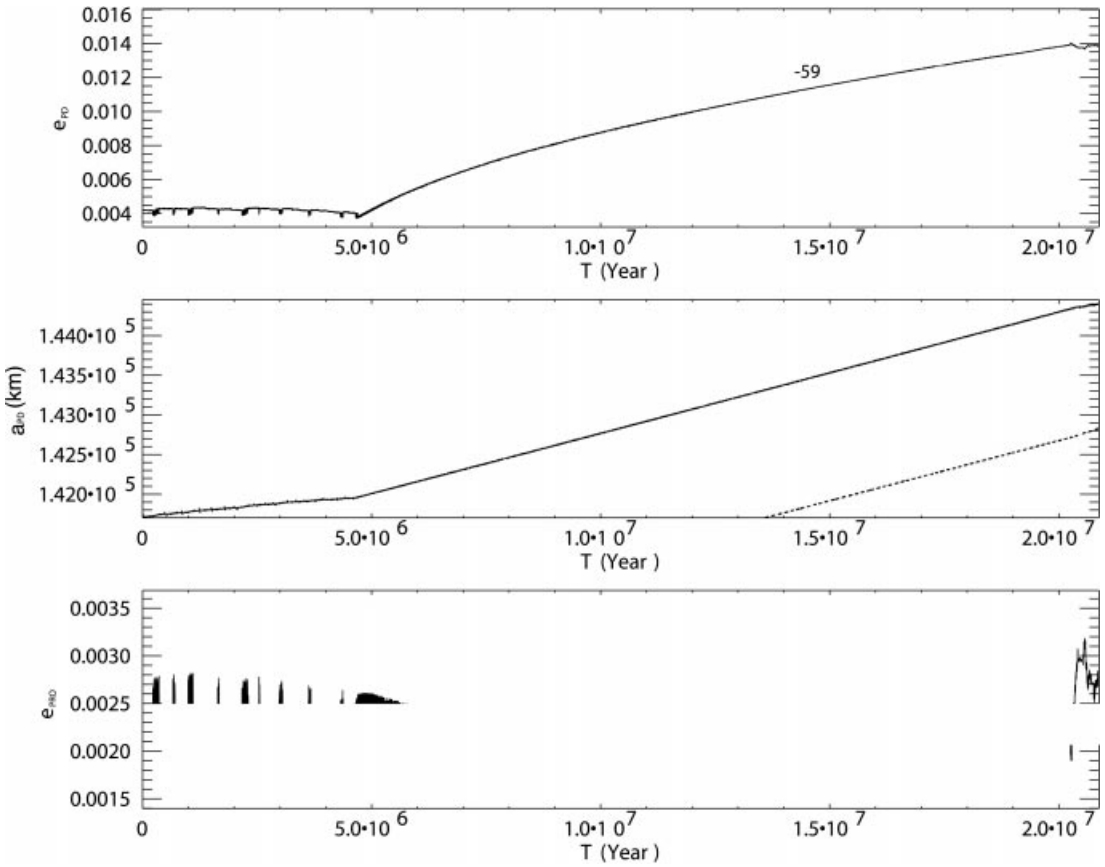

Figure 5. Same as in Fig. 4, but in the case of a capture into the Lindblad resonance, $p = -59$. Note the significant changes in the three parameters at time $T \approx 4.7 \times 10^6$ yr when Pandora gets captured in the resonance. The drift of the semimajor axis of Prometheus is drawn in dashed line in the middle panel. Pandora escapes from the resonance after a capture of $T \approx 15 \times 10^6$ yr, leaving the eccentricity of Pandora at 0.014.

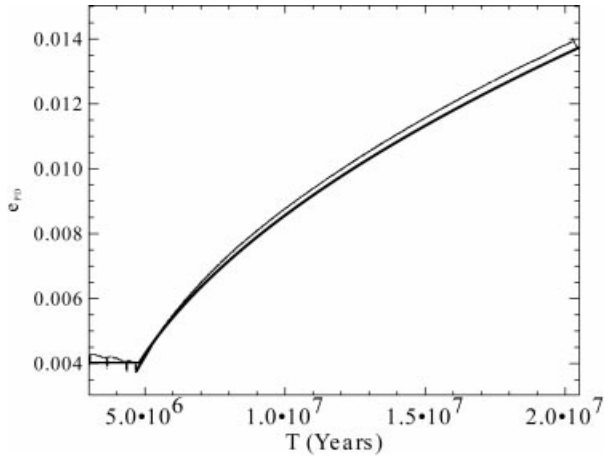

Figure 6. Evolution of the eccentricity of Pandora (thin curve) in isolated, first-order resonance for $p = -59$ (Fig. 5). The thick curve shows the increase in $e_{\rm pd}$ predicted by the low-order analytic theory.

Finally, the history of Pandora during a capture can be summarized in Fig. 8, in which the evolution is followed in the plane $(a_{\rm pd}/a_{\rm pro}, e)$. The motion can be divided into three phases: before, during and after capture. First, there is decrease of $a_{\rm pd}/a_{\rm pro}$, because the semimajor axis of Prometheus increases faster than that of Pandora, which leads Pandora to cross several resonances. During the crossings, its motion is perturbed, and some transient capture can occur, as in the $p = -57$ resonance. Between two resonances, its eccentricity stays constant.

The second stage begins when Pandora encounters the $p = -59$ resonance. Pandora is then trapped. The ratio of the semimajor axes oscillates around a fixed value defined by the exact location of the resonance. However, as mentioned in Section 4.2, the strength of a resonance increases as the square root of the eccentricity. The resonances are weak for small eccentricities and become stronger as the eccentricity increases, i.e., they fill a larger region in the plane $(a_{\rm pd}/a_{\rm pro}, e)$. From a certain eccentricity ($e \approx 8 \times 10^{-3}$ as seen in Fig. 8), the libration regions overlap. Then the overlapping of resonances is generally used as a criterion for the onset of chaotic motion. In the evolution studied here, the trajectory is dragged out toward the chaotic boundary created near the separatrix. This causes a disruption of resonance. We will see below that the mechanism of capture into secondary resonances can accelerate the disruption of the resonant configuration.

The third stage of the motion then begins: Pandora passes through successive resonances ($p = -60, -61, \ldots$) without being captured. None of the simulations showed two successive captures into resonance. At this point, the integration is continued until the moonlets experienced a close encounter.

Role of the secondary resonances: A peculiar behaviour, such as shown in Figs 9 and 10, has been revealed during some captures. It does not change the increase of the eccentricity, but it tends to reduce the lifetime of capture into resonance. Once the

capture is achieved, the eccentricity increases while the ratio of semimajor axis oscillates around the exact location of the resonance in accordance with the adiabatic invariance of the action in the single-resonance theory. However, when the eccentricity of Pandora reaches 0.005 (at $T \approx 9.4 \times 10^6$ yr), the amplitude of libration of ϕ_1 increases. This lasts until the amplitude reaches 2π, at which point there is a disruption of the resonance trapping. This evolution characterizes the capture into secondary resonances.

We benefit from the great amount of past work that has addressed this type of resonance in dynamical studies of the Uranus system (Tittemore & Wisdom 1989; Malhotra & Dermott 1990) and the Neptune system (Banfield & Murray 1992). Secondary resonances are commensurabilities between the libration frequency of a first-order resonance and the circulation frequencies of a neighbouring resonance. The capture into such resonance leads to a destabilization of the orbital resonance, because the trajectory enters near the separatrix of the main resonance. We track this phenomenon in the evolutions of ϕ_1 (Fig. 9) and also $a_{\rm pd}/a_{\rm pro}$ (Fig. 10). When the eccentricity reaches 0.005, the amplitude of oscillation of $a_{\rm pd}/a_{\rm pro}$ decreases before increasing again, and this more strongly than if Pandora stayed in the main first-order resonance. The satellite, captured into secondary resonance, adiabatically evolves along the secondary resonance, and is dragged out towards the boundaries of the first-order resonance. However, the separatrix is a chaotic layer due to the accumulation and overlap of secondary resonances, and the satellite which is forced into such a chaotic layer is expected to escape from the resonant configuration. After escape, the third stage of the evolution begins: Pandora continues to cross through

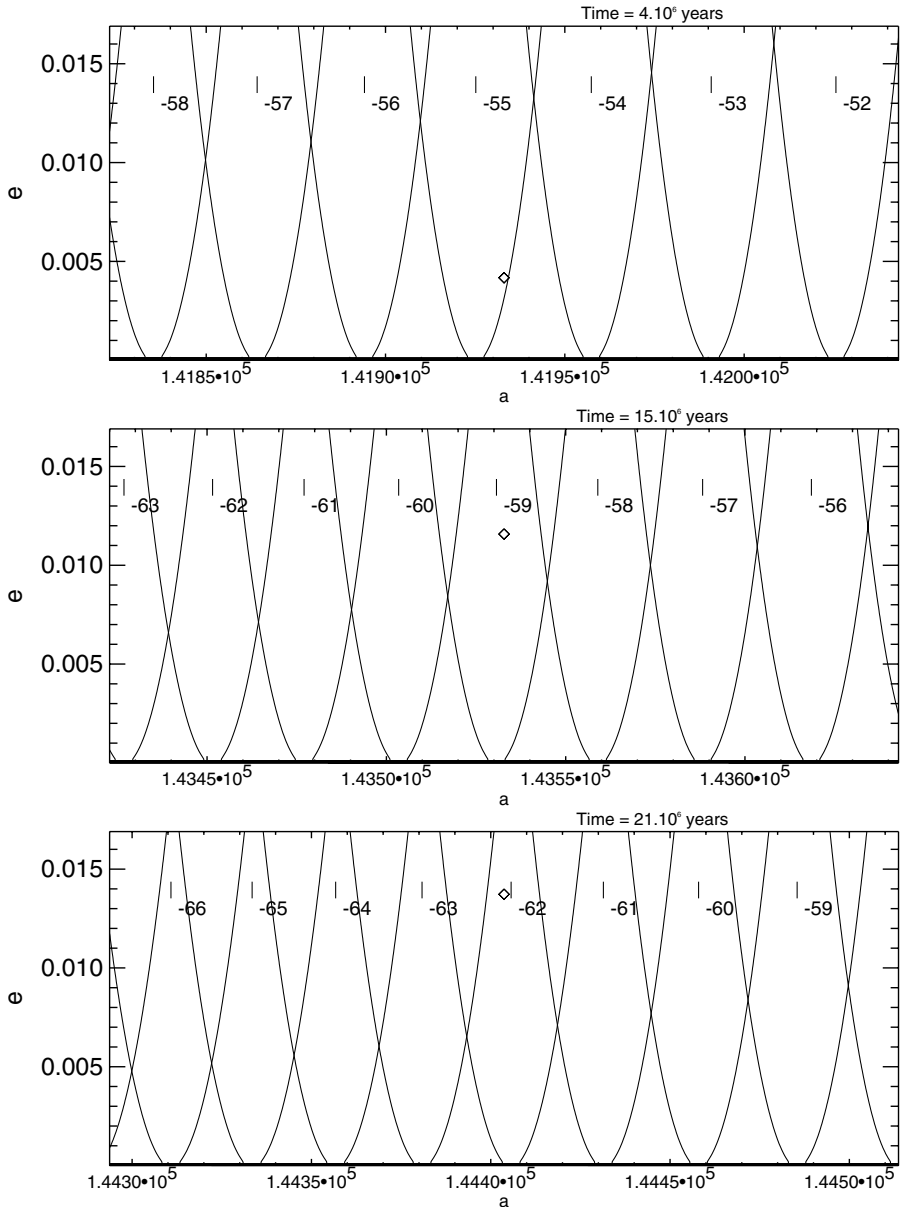

Figure 7. Evolution of the trajectory of Pandora seen in Fig. 5 in the diagram (a, e). The V-shaped curves define the eccentric Lindblad resonances. The resonances move radially from left to right relative to Pandora identified by a diamond. The three snapshots taken at three different times show the position of the satellite before the capture ($T = 4 \times 10^6$ yr, top panel), in resonance ($T \approx 15 \times 10^6$ yr, middle panel), and after its escape ($T \approx 21 \times 10^6$ yr, bottom panel). When the satellite is trapped into resonance, the eccentricity is pumped.

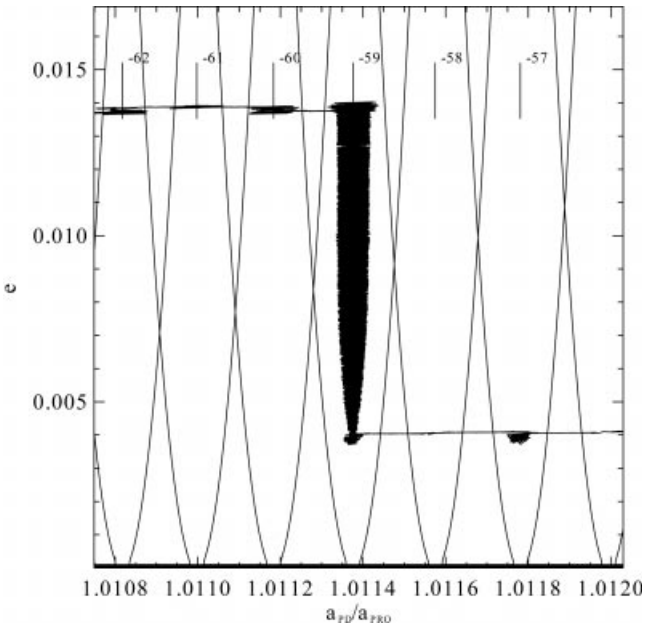

Figure 8. Representation of the numerical experiment shown in Fig. 5 in the plane $(a_{\rm pd}/a_{\rm pro}, e)$. With t increasing, we see clearly that (1) the trajectory first passes through the resonances $p = -57, -58$ without being captured; (2) it then gets captured in the -59 resonance leading to an increase of $e_{\rm pd}$; (3) it escapes from the resonance because of the overlapping of resonances.

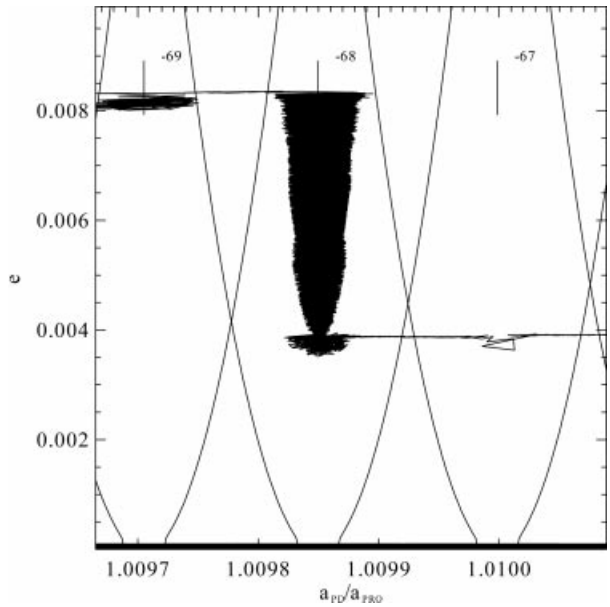

Figure 10. Evolution of $a_{\rm pd}/a_{\rm pro}$ for the evolution shown in Fig. 9. The evolution reads from right to left. The effect of the capture into secondary resonance is detected from the eccentricity 0.005, where the amplitude of the libration increases such that the trajectory is rushed toward the chaotic boundary of the first-order resonances. The trajectory escapes from the resonance, and continues to cross other resonances.

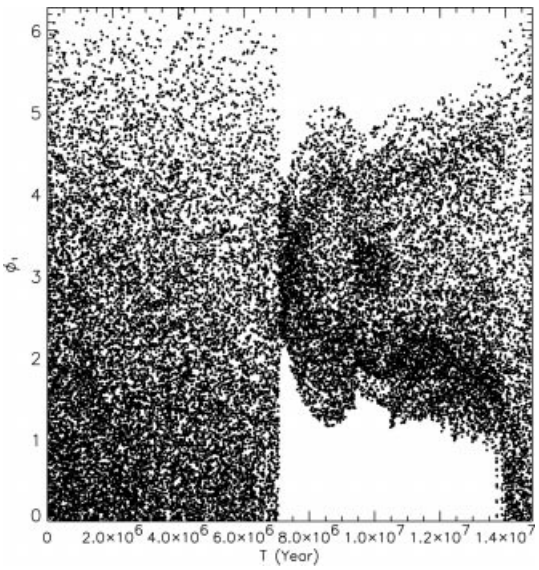

Figure 9. A typical example of the behaviour of the libration angle in a secondary resonance. Before capture, ϕ_1 circulates. Once capture into a first-order resonance occurs (at about $T \approx 7 \times 10^6$ yr), ϕ_1 oscillates around 180°. A significant change in the behaviour occurs at $T \approx 9.4 \times 10^6$ yr, when the amplitude of ϕ_1 begins to increase. The trajectory encounters a secondary resonance. The amplitude continues to increase, and eventually there is disruption of the resonant configuration. After that, ϕ_1 circulates again.

the resonances with an eccentricity of order of 0.008. Fig. 11 shows the continuation of the numerical integration. The behaviour becomes more and more irregular, and can be described as chaotic.

7 LIFETIME OF PROMETHEUS–PANDORA SYSTEM

The previous work was motivated by the search for stable resonant configurations of the Prometheus–Pandora system. We showed that some commensurable orbits could be formed. In order to obtain statistical results on these evolutions, some 40 simulations have been done for each set of considered masses ($\rho = 0.6$ and $1.2\,{\rm g\,cm^{-3}}$). The simulations differ by their rate of orbital expansion, between 0.9 and 1.1 times the nominal value derived from equations (1) and (2). The results are shown in Figs 12 and 13 which present the probability of capture and the distribution of lifetime, respectively.

For each set of masses, all the simulations added together corresponds to about 1000 crossings through resonances (from $p = -41$ to $p = -70$). The process of capture depends on $e_{\rm pd}$ before the crossing, but on average $e_{\rm pd} \sim 0.004$. The probabilities of capture into one resonance derived from the numerical integrations are compared with the analytic estimates (equation 19). Under the hypothesis of the single-resonance theory (adiabatic motion and isolated resonance), we find that the probability of capture is in very good agreement with the analysis. However, some captures occur when the resonances were not well separated. This effect increases the number of capture by about 75 per cent. Note that the results are quantitatively the same for each mass.

A capture into resonance allows the avoidance of a close encounter, which usually occurs after 10 Myr (20 Myr for densities 2 times smaller). In that case, a certain stability can be obtained for several tens of Myr. Once Pandora is ejected from the resonance, the orbital convergence ends by a chaotic motion. Eventually, a close encounter occurs, but it is not studied numerically here, because the symplectic integration validity

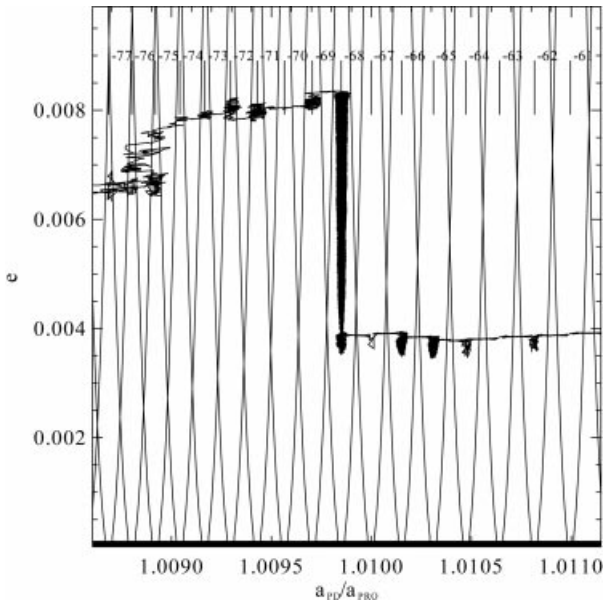

Figure 11. A broader view of the evolution of $a_{\rm pd}/a_{\rm pro}$ as showed in Fig. 10. The evolution reads from right to left. After the disruption of the resonance, the trajectory becomes unpredictable because of the overlap of resonances for eccentricities larger than a few times 10^{-3}.

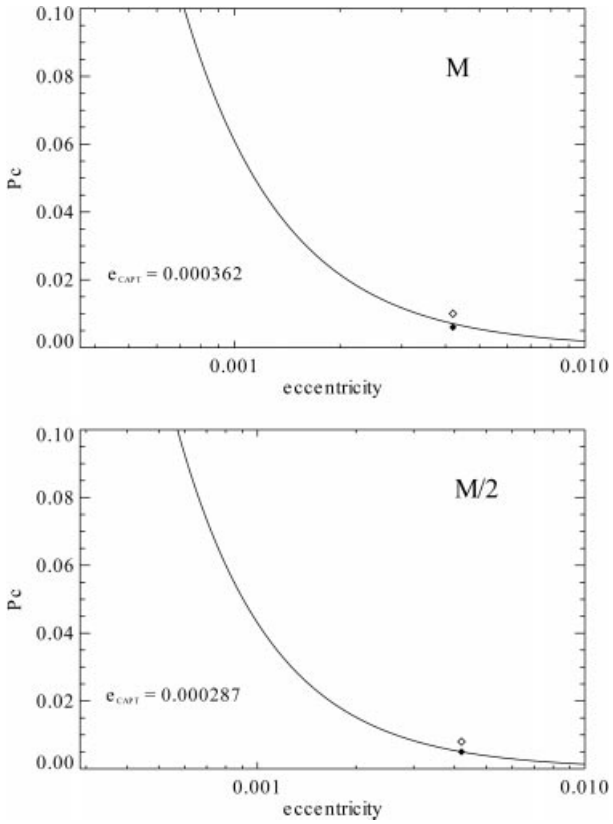

Figure 12. Probability of capture into isolated resonance for two densities: 1.2 g cm^{-3} (upper panel) and 0.6 g cm^{-3} (lower panel). The curves derived from equation (19) are compared with the numerical results represented by diamonds. The filled diamond represents the probability of capture into one isolated resonance from the runs (about 40). The open diamond represents the total probability (1 per cent) of capture in one resonance even if it is not isolated. The analytic probabilities are computed for the $p = -50$ resonance. The value of the eccentricity for a certain capture (equation 17) is indicated for each set of mass.

breaks down. Let us define the 'lifetime' as the time of the orbital evolution from the present time to a close encounter. Fig. 13 shows the distribution of lifetime for about 40 simulations and for each set of mass. We classify our results in terms of evolution without or with capture. In 25 per cent of the simulations, Pandora is trapped in a resonance. The lifetime of the system can then reach several tens Myr (the maximal observed lifetime being 75 Myr), against only a 10 Myr for a typical evolution without capture. The results are similar for the density of 0.6 g cm^{-3} except for a typical lifetime of evolution without capture of about 20 Myr.

Finally, a close approach between the shepherd satellites seems to be inescapable. The physics of an encounter has been formulated in the three-body problem (Petit & Hénon 1986; Ida & Kanazawa 1989; Ida & Nakazawa 1989). In most cases, the orbits of the two bodies are unstable, and they probably evolve into physical collision. The collisionnal velocity could be large enough to fragment the satellites and to disperse the fragments into individual orbits. The physics of such event is beyond the purpose of its paper, but the consequences of such an evolution (orbital convergence of two satellite following by catastrophic collision) on the formation of rings are discussed below.

8 CONCLUSIONS

We studied the dynamic behaviour of Saturn's inner satellites. The role of the eccentric first-order resonances on the evolution of the shepherd satellites, Prometheus–Pandora, is presented. Because of resonances with the rings, these satellites extract angular momentum from the ring system, and therefore they should evolve outward at different rates of orbital expansion. This leads to an age on the order of 20 Myr for these satellites. Their lifetime could be significantly larger if they are captured into resonance.

The most efficient resonances are defined by commensurabilities $p + 1 : p$ ($p < 0$). The probability of capture is about 25 per cent. A capture increases the lifetime of the satellites by an order of magnitude at most, but the mechanism of capture is not efficient enough for the satellites to avoid a close encounter during time-scale typical of the age of the Solar system. We observe spontaneous disruptions of resonances leading to a chaotic motion because of the strong overlapping of resonances. The orbital convergence ends by a close encounter.

The problem of the long-term evolution of these satellites is directly linked to that of the age of Saturn's rings. The physical phenomena which actually sculpt the Saturn's rings in long-term have time-scales lower than a few tens of Myr. Two scenarios of formation of Saturn's rings have been generally considered by various authors to explain the problem of the short time-scale. The first consists of a catastrophic destruction of an inner satellite by cometary impact (Esposito 1986), the second of the destruction of a comet during a close encounter with Saturn (Dones 1991). However, it is well recognized that these events were unlikely during the last hundred Myr (Lissauer, Squyres & Hartmann 1988; Dones 1991; Colwell 1994; Colwell, Esposito & Bundy 2000).

We discuss here about a new scenario: *Recurrent collisions between inner ring moons have replenished the rings. Satellites entered into collisions following orbital convergences similar to the case of Prometheus and Pandora.* Each physical collision between satellites could disrupt them into several large fragments

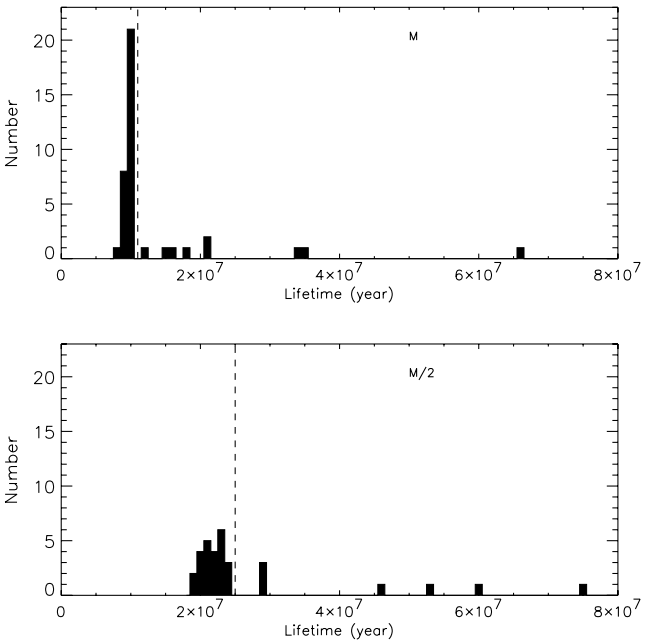

Figure 13. Distribution of lifetime of the system before a close encounter for the two considered densities. In 25 per cent of the runs, there is a capture of Pandora in a Lindblad resonance. In these cases, the lifetime of the system is significantly increased and can reach several tens of Myr. The vertical dashed lines separate the runs without captures (left) from the runs with captures (right).

plus multiple small particles. The largest fragments, that we call satellites, are pushed outward by exchange of angular momentum with the existing rings until a new collision between two satellites occurs. This creates either new ring particles by catastrophic collision or a larger satellite by accretion. The age of the rings since the last collision is then derived by the time-scale of the tidal evolution of the small moons. An estimate comes from the long-term stability of Prometheus and Pandora which could reach several tens of millions of years. If this type of evolution has been recurrent, the age of the rings could then be greater than 100 Myr. This would revalidate the scenario of initial rings formation by disruption of a satellite or a comet.

However, there are some unknowns in this model. If the initial contribution came from a satellite disruption, this had at least a mass comparable to that of Mimas. The low mass of the actual inner satellites (about half of the mass of A ring) tends to indicate that we see the late stages of this process of regeneration. They would no longer have enough material to replenish the rings, unless some moons reaccrete again from the actual rings. Moreover, there are many unsolved questions in the stage of the collision between two satellites: Are collisions catastrophic? Can the energy of disruption be large enough to prevent the reaccretion of the fragments into gravitationaly bound rubble pile? How do create centimetre-sized particles from bodies several tens of kilometres in size? We plan to make further efforts in these directions.

ACKNOWLEDGMENTS

We thank C. D. Murray and J. M. Petit for useful discussions. This work was supported by the French Programme National de Planétologie, by the Université Paris IV, and by the North American National Research Council.

REFERENCES

Banfield D., Murray N., 1992, Icarus, 99, 390
Borderies N., Goldreich P., 1984, Celest. Mech., 32, 127
Borderies N., Goldreich P., Tremaine S., 1984, in Greenberg R., Brahic A., eds, Planetary Rings. Univ. Arizona, Tucson, p. 713
Brophy T. G., Esposito L. W., Stewart G. R., Rosen P. A., 1992, Icarus, 100, 412
Burns J. A., 1977, in Burns J. A., eds, Planetary Satellites. Univ. Arizona, Tucson, p. 113
Campbell J. K., Anderson J. D., 1989, AJ, 97, 1485
Colwell J. E., 1994, Planet. & Space Sci., 42, 1139
Colwell J. E., Esposito L. W., Bundy D., 2000, J. Geophys. Res., 105, Issue E7, 17 589
Cuzzi J. N., Burns J., 1988, Icarus, 74, 284
Cuzzi J. N. et al., 1984, in Greenberg R., Brahic A., eds, Planetary Rings. Univ. Arizona, Tuscon, p. 73
Dermott S. F., Murray C. D., 1983, Nat, 301, 201
Dermott S. F., Malhotra R., Murray C. D., 1988, Icarus, 76, 295
Dones L., 1991, Icarus, 92, 194
Dones L., Showalter M. R., French D., Lissauer J. J., 1999, BAAS, 31, 1228
Duncan M. J., Lissauer J. J., 1997, Icarus, 125, 1
Esposito L. W., 1986, Icarus, 67, 345
Foryta D. W., Sicardy B., 1996, Icarus, 123, 129 (FS96)
French D. et al., 1998, BAAS, 30, 1141
French D., McGhee C. A., Nicholson P. D., Dones L., Lissauer J., 1999, BAAS, 31, 1228
Goldreich P., 1965, MNRAS, 126, 257
Goldreich P., Tremaine S., 1982, ARA&A, 20, 249
Henrard J., Lemaître A., 1983, Celest. Mech., 30, 197
Ida S., Nakazawa K., 1989, A&A, 224, 303
Lissauer J. J., Peale S. J., Cuzzi J. N., 1984, Icarus, 58, 159
Lissauer J. J., Goldreich P., Tremaine S., 1985, Icarus, 64, 425
Lissauer J. J., Squyres S. W., Hartmann W. K., 1988, J. Geophys. Res., 93, 13776
Malhotra R., Dermott S. F., 1990, Icarus, 85, 444
Murray C. D., Giuliatti Winter S. M., 1996, Nat, 380, 139
Nicholson P. D., Hamilton D. P., Matthews K., Yoder C. F., 1992, Icarus, 100, 464
Nicholson P. D. et al., 1996, Sci, 272, 509
Peale S. J., 1986, in Burns J. A., Matthews M. S., eds, Satellites. Univ. Arizona, Tucson, p. 159
Petit J. M., Hénon M., 1986, Icarus, 66, 536
Poulet F., Jancart S., 2000, DDA, 32, 7
Poulet F., Sicardy B., Nicholson P. D., Karkoschka E., Caldwell J., 2000, Icarus, 144, 135
Rosen P. A., Tyler G. L., Marouf E. A., Lissauer J. J., 1991, Icarus, 93, 25
Scargle ?. et al., 1993, BAAS, 25, 1003
Schubert G., Spohn T., Reynolds R., 1986, in Burns J. A., Matthews M. S., eds, Satellites. Univ. Arizona, Tucson, p. 224
Showalter M. R., Dones L., Lissauer J., 1999, BAAS, 31, 1228
Synnott S. P. et al., 1983, Icarus, 53, 156
Tittemore W. C., Wisdom J., 1988, Icarus, 74, 172
Tittemore W. C., Wisdom J., 1989, Icarus, 78, 63
Winter O. C., Murray C. D., 1997, A&A, 319, 290

This paper has been typeset from a TEX/LATEX file prepared by the author.